

# LINEAR MHD WAVES IN PENUMBRAL STRUCTURES

A. Marcu<sup>1</sup> and I. Ballai<sup>2</sup>

<sup>1</sup> Centre for Research in Space Plasmas, Dept. of Theoretical and Computational Physics, Babes-Bolyai University, 1, M. Kogalniceanu, 3400 Cluj-Napoca, Romania

<sup>2</sup> SPARG, Dept. of Applied Mathematics, University of Sheffield, Hicks Building, Hounsfield Road, Sheffield, S3 7RH, England (UK)

E-mail: <sup>1</sup>amarc@phys.ubbcluj.ro, <sup>2</sup>i.ballai.sheffield.ac.uk

## Abstract

In this paper we study the oscillations of a magnetic medium periodic in the x-direction with B parallel to z in the presence of a steady equilibrium field aligned flow. The case with no gravity and stepwise profile for B(x), allowing a normal mode analysis, is studied and the dispersion relation for linear compressional waves is derived. The propagation of waves is studied in particular case modelling the propagation of waves in the penumbral filamentary structures in the photosphere.

**Keywords:** *Sun: magnetohydrodynamics(MHD) waves, Sun: magnetic field*

## 1 Introduction

The recent observational evidence for the existence of waves and oscillations in the solar atmosphere has invigorated theoretical developments in this field. Waves are responsible for carrying energy and momentum, creating instabilities, generating phenomena like magnetic reconnection, phase mixing, etc. They can serve as a unique tool for plasma diagnostics due to their capability of carrying information about the medium in which they propagate.

Solar and space plasmas have a very dynamic character, showing steady flow on all sorts of time and space scales. This property is confirmed by recent ground and space-born satellite observations. Steady flows have been observed in the photosphere, chromosphere (November et al. 1979, Athay and Dere 1991), corona (Winebarger et al. 2002) and beyond, in the solar wind (Gabriel et al. 2003). Therefore, theoretical

models should include the presence of an equilibrium steady flow. Equilibrium flows are known to introduce a series of new effects such as Kelvin-Helmholtz and resonant instabilities, negative energy waves, etc.

Observations have also revealed that the solar plasma is structured and this is determined and controlled by the magnetic field. In the photosphere, the magnetic field is concentrated in thin flux tubes with field strengths exceeding 1000 G (Spruit 1981). The flux tubes extend well into the chromosphere and corona contributing to the net heating of the solar upper layers, creating solar spicules (Roberts 1979, James and Erdélyi 2002) and even contributing to the solar wind acceleration.

Many solar features (e.g. the granular pattern in the photosphere, the penumbra, plume/interplume, etc.) show a transversal periodicity (or quasi-periodicity). Waves propagating along magnetic structures with a transversal periodicity is likely to 'feel' the effect of this structure provided their transversal wavelength is of the same order as the transversal spatial organisation scale. Effects of periodicity, though it is not perfect on the Sun's surface, could possibly be observationally detected on diagnostic  $\omega$ - $k$  diagram. The possibility of wave propagation in a periodic structure has been discussed by Hollweg (1982), Berton and Heyvaerts (1987) and Uralov (2003) in the linear regime, while the steepening of linear waves into nonlinear waves (solitons) in periodic structures has been studied by Hollweg and Roberts (1984) and Ruderman et al. (2001).

Here we present some preliminary results on the propagation of compressional MHD waves in a magnetically periodical structure with field aligned flow. Weak field regions alternate with strong field regions modelling the filamentary structure of the penumbra.

## 2 Derivation of Dispersion Relations

We consider an ideal, perfectly conducting fluid permeated by a magnetic field of constant direction along the  $z$ -axis, and periodic along the  $x$ -axis. We suppose that the wavelengths are smaller than the gravitational scale-height, i.e. gravitational effects are neglected.

A field-aligned equilibrium steady flow is present in the system. In the present paper we suppose that the medium consists of alternating magnetic slabs (with width  $L_i$  and  $L_e$ ) with homogeneous magnetic fields inside them ( $B_i$  and  $B_e$ , with  $B_i > B_e$ ) and sharp discontinuities at the boundaries. Let us denote by  $L = L_i + L_e$  the periodicity of the medium. The continuity of the total pressure at each boundary requires an equation of the type

$$\frac{d}{dx} \left( p_0 + \frac{B_0^2}{2\mu} \right) = 0, \quad (1)$$

which, in particular, leads to a density contrast in two adjacent regions

$$\frac{\rho_i}{\rho_e} = \frac{2c_{0e}^2 + \gamma c_{Ae}^2}{2c_{0i}^2 + \gamma c_{Ai}^2}, \quad (2)$$

where  $c_{0i,e}$  and  $c_{Ai,e}$  denote the sound and Alfvén speeds in the two layers,  $\gamma$  is the adiabatic index and  $\mu$  is the magnetic permeability.

We perturb the system of linearized ideal MHD equations and write all physical quantities in the form  $f_0 + f$  where  $f_0$  are the equilibrium values and  $f$  their Eulerian perturbations. Since the equilibrium quantities depend on  $x$  only, we write all perturbations as

$$f = \hat{f}(x)e^{i(\omega t - k_z z)}.$$

The dispersion relation of linear compressional MHD waves can be written as (Roberts 1981)

$$\frac{d^2 \hat{v}_x}{dx^2} - q^2 \hat{v}_x = 0, \quad (3)$$

where the magnetoacoustic parameter,  $q^2$  is defined as

$$q(x)^2 = \frac{(k_z^2 c_A^2 - \Omega^2)(k_z^2 c_0^2 - \Omega^2)}{(c_0^2 + c_A^2)(k_z^2 c_T^2 - \Omega^2)}, \quad (4)$$

with  $\Omega = \omega - k_z v_0$  being the Doppler-shifted frequency and  $c_T = c_0 c_A / (c_0^2 + c_A^2)^{1/2}$  the tube (cusp) velocity. The quantity  $q^2$  is constant in each region and it can take both, positive and negative values.

The solutions of Eq. (3) inside and outside the slab can be written as

$$\begin{cases} \hat{v}_{xi} = \alpha_i e^{q_i x} + \beta_i e^{-q_i x} \\ \hat{v}_{xe} = \alpha_e e^{q_e x} + \beta_e e^{-q_e x} \end{cases} \quad (5)$$

where the coefficients  $\alpha_i$ ,  $\beta_i$ ,  $\alpha_e$  and  $\beta_e$  are four constants which can be determined by matching conditions at the boundaries of two adjacent regions (at  $x = L_i/2$  and  $x = L_e + L_i/2$ ). Due to the periodicity of the medium we employ a method widely used in solid state physics. We introduce the quantity  $K_0$  (called the *Bloch wavenumber*) which plays the same role as the wavenumber  $k_x$  in a homogeneous medium. According to the Bloch's theorem, a solution of the Eq. (3) which is bounded at infinity can be written as

$$\hat{v}_x = aF(x)\exp[iK_0 x] + bF(-x)\exp[-iK_0 x], \quad (6)$$

where  $F(x)$  is a periodic function with the period  $L$ . Then

$$\frac{\hat{v}(L)}{\hat{v}(0)} = \cos K_0 L.$$

In the case of surface ( $q_i^2 > 0$ ) and body ( $q_i^2 < 0$ ) modes, the dispersion relations can be written as

$$\cos(K_0 L) = \cosh(\theta_i) \cosh(\theta_e) + \frac{1}{2} \left( S + \frac{1}{S} \right) \sinh(\theta_i) \sinh(\theta_e), \quad (7)$$

$$\cos(K_0 L) = \cos(\theta_i) \cosh(\theta_e) + \frac{1}{2} \left( S - \frac{1}{S} \right) \sin(\theta_i) \sinh(\theta_e), \quad (8)$$

$$S = \frac{\rho_i q_e k_z^2 c_{Ai}^2 - \Omega_i^2}{\rho_e q_i k_z^2 c_{Ae}^2 - \Omega_e^2}. \quad (9)$$

The dispersion curves  $\omega(k_z)$  will depend upon the Bloch's wave number,  $K_0$ , as a parameter.

According to the relative magnitude of the characteristic speeds  $c_0$ ,  $c_A$ , and  $c_T$  in the internal and external regions, various situations are possible depending on the signs of the quantities  $q_i^2$  and  $q_e^2$ . For a simpler representation it is convenient to use the following dimensionless quantities

$$R_\rho = \frac{\rho_i}{\rho_e}, \quad R_T = \frac{T_i}{T_e}, \quad R_B = \frac{B_i}{B_e}, \quad R_L = \frac{L_i}{L_e}, \quad (10)$$

where  $T_i$  and  $T_e$  denote the temperatures in the two regions. In these new notations, Eq. (2) can be rewritten as

$$\frac{c_{0i}^2}{c_{Ai}^2} = \frac{\gamma R_\rho R_T}{2} \frac{R_B^2 - 1}{1 - R_\rho R_T}. \quad (11)$$

In what follows, the dispersion relations are solved for incompressible and compressible plasmas.

## 2.1 Incompressible Modes

A first insight into the properties of the possible modes propagating in periodic plasma structures can be acquired by considering the incompressible plasma limit which yields a relatively simple analytical solution. This solution enables us to gain a better understanding of the behaviour of the different modes with respect to the equilibrium steady flow. For an incompressible plasma ( $\gamma \rightarrow \infty$ )  $q^2(x) = |k_z| > 0$ , i.e. only surface trapped modes are allowed to propagate. The dispersion relation of surface waves (Eq. (7)) becomes

$$\cos \Phi = \cosh(\theta) \cosh\left(\frac{\theta}{R_L}\right) + \frac{1}{2} \left( S + \frac{1}{S} \right) \sinh(\theta) \sinh\left(\frac{\theta}{R_L}\right) \quad (12)$$

where

$$S = R_\rho \frac{c_{Ai}^2 - (c - v_{0i})^2}{c_{Ae}^2 - (c - v_{0e})^2}, \quad \theta = k_z L_i, \quad \Phi = K_0 L. \quad (13)$$

and  $c = \omega/k_z$  is the phase speed of the waves. The numerical investigation of these modes requires the function  $c(\theta)$  satisfies Eqs. (12) and (13), where  $\Phi$  is a parameter. Inverting Eq. (12) yields

$$S^2 - 2 \frac{\cos \Phi - \cosh(\theta) \cosh(\frac{\theta}{R_L})}{\sinh(\theta) \sinh(\frac{\theta}{R_L})} S + 1 = 0 = S^2 - 2US + 1, \quad (14)$$

with

$$\frac{\cos \Phi - \cosh(\theta) \cosh(\frac{\theta}{R_L})}{\sinh(\theta) \sinh(\frac{\theta}{R_L})} = U. \quad (15)$$

Using this notation, Eq. (14) can have two roots

$$S_{\pm} = U \pm \sqrt{U^2 - 1}, \quad (16)$$

where the  $\pm$  sign corresponds to sausage and kink modes, respectively. In Eq. (16) we have to impose that  $U^2 \geq 1$ , i.e. the quantity  $S$  is real. Since

$$S = \frac{c_{Ai}^2 - (c - v_{0i})^2}{c_{Ae}^2 - (c - v_{0e})^2} R_{\rho}, \quad (17)$$

the dispersion relation of fast magnetoacoustic modes propagating in periodic structures in incompressible limit is given by the roots of

$$c^2(R_{\rho} - S_{\pm}) + 2c(S_{\pm}v_{0e} - R_{\rho}v_{0i}) - R_{\rho}(c_{Ai}^2 - v_{0i}^2) + S_{\pm}(c_{Ae}^2 - v_{0e}^2) = 0. \quad (18)$$

Eq. (18) posses two real roots corresponding to two possible sausage or kink modes provided

$$\frac{R_{\rho}S}{R_{\rho} - S} > \frac{Sc_{Ae}^2 - R_{\rho}c_{Ai}^2}{(v_{0i} - v_{0e})^2}$$

If the two equilibrium flow speeds are set to be zero we recover the results by Berton and Heyvaerts (1987).

Before turning to the general case, let us first discuss two particular cases, i.e  $R_L \rightarrow 0$  (the isolated slab) and  $R_L \rightarrow \infty$  (homogeneous plasma). In the case of an isolated tube,  $U = -\coth \theta$ , so the phase speed of fast surface sausage modes is given by

$$c_+^2 - 2c_+ \frac{v_{0e} \tanh \frac{\theta}{2} + v_{0i} R_{\rho}}{\tanh \frac{\theta}{2} + R_{\rho}} - \frac{(c_{Ae}^2 - v_{0e}^2) \tanh \frac{\theta}{2} + (c_{Ai}^2 - v_{0i}^2) R_{\rho}}{\tanh \frac{\theta}{2} + R_{\rho}} = 0, \quad (19)$$

while the propagation speed of fast surface kink modes is described by

$$c_+^2 - 2c_+ \frac{v_{0e} \coth \frac{\theta}{2} + v_{0i} R_{\rho}}{\coth \frac{\theta}{2} + R_{\rho}} - \frac{(c_{Ae}^2 - v_{0e}^2) \coth \frac{\theta}{2} + (c_{Ai}^2 - v_{0i}^2) R_{\rho}}{\coth \frac{\theta}{2} + R_{\rho}} = 0, \quad (20)$$

identical to the results obtained by Nakariakov and Roberts (1995). This form of Eqs. (19) and (20) allows us to interpret the effect of the equilibrium flow. In both equations, the second terms owe their existence to the equilibrium internal and external flows.

In the limit of homogeneous plasma, we let  $R_L \rightarrow \infty$  and we obtain the well-known propagation speeds for sausage and kink modes

$$c_+ = \pm c_{Ai} + v_{0i}, \quad c_- = \pm c_{Ae} + v_{0e} \quad (21)$$

where here the  $\pm$  indicates forward (parallel to the magnetic field) and backward (anti-parallel to the magnetic field) propagation.

In the general case we can derive analytical solution for the phase speed of sausage and kink modes propagating in the incompressible periodic plasma in two extreme limits corresponding to thin ( $\theta \ll 1$ ) and thick ( $\theta \gg 1$ ) slab.

In a thin slab,  $U$  can be approximated as

$$U \sim -\frac{2R_L}{\theta^2} \sin^2 \frac{\Phi}{2}, \quad (22)$$

which in the case of  $\theta \rightarrow 0$  leads to the approximate expressions

$$S_+ \sim \frac{1}{2U}, \quad S_- \sim 2U. \quad (23)$$

These expressions can now be used to obtain the phase speed of fast sausage and kink modes as

$$c_+^2 - 2c_+ \frac{4 \frac{R_L R_\rho}{\theta^2} \sin^2 \frac{\Phi}{2} v_{0i} + v_{0e}}{1 + 4 \frac{R_L R_\rho}{\theta^2} \sin^2 \frac{\Phi}{2}} - \frac{4 \frac{R_L R_\rho}{\theta^2} \sin^2 \frac{\Phi}{2} (c_{Ai}^2 - v_{0i}^2) + c_{Ae}^2 - v_{0e}^2}{1 + 4 \frac{R_L R_\rho}{\theta^2} \sin^2 \frac{\Phi}{2}} \quad (24)$$

and

$$c_-^2 - 2c_- \frac{4 \frac{R_L}{\theta^2} \sin^2 \frac{\Phi}{2} v_{0e} + v_{0i} R_\rho}{R_\rho + 4 \frac{R_L}{\theta^2} \sin^2 \frac{\Phi}{2}} - \frac{4 \frac{R_L}{\theta^2} \sin^2 \frac{\Phi}{2} (c_{Ae}^2 - v_{0e}^2) + R_\rho (c_{Ai}^2 - v_{0i}^2)}{R_\rho + 4 \frac{R_L}{\theta^2} \sin^2 \frac{\Phi}{2}} \quad (25)$$

In the wide slab limit,  $S_\pm \rightarrow -1$  and the dispersion relation is given by

$$c_\infty^2 - 2c_\infty \frac{v_{0e} + v_{0i} R_\rho}{R_\rho + 1} - \frac{R_\rho (c_{Ai}^2 - v_{0i}^2) + c_{Ae}^2 - v_{0e}^2}{R_\rho + 1} = 0 \quad (26)$$

The possible modes propagating in a incompressible periodic structure for an arbitrary  $\theta$  and  $R_L$  are shown in Figure 1. All characteristic speeds are expressed in units of the internal Alfvén speeds and the following notations have been used

$$a = \frac{c_{Ae}}{c_{Ai}}, \quad M_i = \frac{v_{0i}}{c_{Ai}}, \quad M_e = \frac{v_{0e}}{c_{Ai}}.$$

Figure 1 depicts the possible modes propagating in a periodic structure when no plasma flow is present in the system.

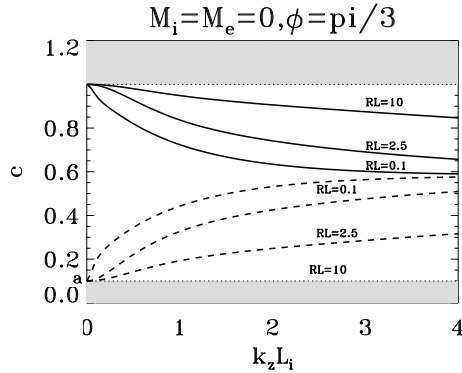


**Figure 1:** The phase speed of sausage (solid line) and kink modes (dashed lines) as a function of the dimensionless wavelength,  $\theta$  for an incompressible periodic plasma with  $a = 10$  and  $a = 1$  and  $M_i = M_e = 0$ .

As expected, these modes are identical to the results obtained by Berton and Heyvaerts (1987). Since the equilibrium state is static, the modes are symmetric with respect to the horizontal axis, therefore in Figure 1 we plot only the forward propagating modes. The possible modes are allowed to propagate between the two Alfvén speeds, the grey regions are the intervals where waves become leaky. The phase speed given by the dispersion relation has been plotted for  $\Phi = \pi/3$  and for three different values of  $R_L$  (0.1, 2.5, 10). A simple visual inspection shows that waves are more dispersive for small values of  $R_L$ , i.e. for transversal dimensions of the adjacent slabs close to each other. The phase speed of both types of waves is increasing with increasing the  $R_L$  number. In general, sausage waves (with positive dispersion) propagate faster than kink modes (with negative dispersion). For large values of  $\theta$  both, sausage and kink modes will tend towards the positive value of  $c_\infty$  given by Eq. (26).

When an equilibrium flow is taken into account (Figures 2-3) the symmetry of the modes is broken although the propagation windows of the forward and backward propagating modes are shifted by an amount proportional to the flow speed. Figures 2 and 3 were obtained for two values of  $\Phi(0, \pi/2)$  and for three different values of  $R_L$  (0.1, 2.5, 10). We have considered the case  $R_B > 1$  with  $a = 0.1$  and  $R_p = 0.5$ ,  $M_i = 0.04$  and  $M_e = -0.02$ .

Repeating the plotting for other values of  $\Phi$ , we can observe that the dependence of the phase speed on  $\theta$  is very similar to the case obtained for  $\Phi = \pi/2$ , only small changes are observed for intermediate values of  $\theta$ . When  $\Phi = 0$ , sausage and kink

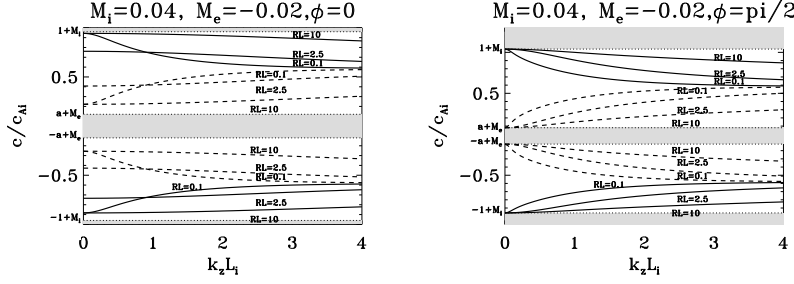


**Figure 2:** The same as in Figure 1 but now  $M_i = 0.04$ ,  $M_e = -0.02$  and  $\Phi = 0$  (left panel) and  $\Phi = \pi/2$  (right panel)

modes show a significant dispersion for small values of  $R_L$ , and for values greater than 1, waves are weakly dispersive. When  $\Phi \neq 0$  the behaviour of oscillating modes is similar to the case obtained in a static equilibrium.

## 2.2 Compressible modes

The dispersion relations for surface and body modes have a rich variety of solutions. In what follows we only the slender-slab ( $\theta \ll 1$ ) approximation.

Surface modes propagate with phase speeds given by the dispersion relation (7), which in the  $\theta \ll 1$  limit reduces to

$$-\frac{4 \sin^2 \frac{\Phi}{2}}{\theta^2} \approx q_i^2 + \frac{q_e^2}{R_L^2} + \left(S + \frac{1}{S}\right) \frac{q_i q_e}{R_L}. \quad (27)$$

If  $\Phi \neq 0$ , the two possible modes propagate with phase speeds given by

$$c \approx v_{0i} \pm c_{Ti} \left\{ 1 + \frac{c_{Si}^2}{c_{Ai}^2 c_i^2} \left[ R_L R_\rho \frac{c_{Ai}^4}{c_i^2} + c_{Ae}^2 - (v_{0i} \pm c_{Ti} - v_{0e})^2 \right] \frac{\theta^2}{8 \sin^2 \frac{\Phi}{2} R_L R_\rho} \right\} \quad (28)$$

and

$$c \approx v_{0e} \pm c_{Te} \left\{ 1 + \frac{c_{Se}^2}{c_{Ae}^2} \left[ \frac{c_{Ae}^4}{c_e^2} \frac{1}{R_L R_\rho} + c_{Ai}^2 - (v_{0e} \pm c_{Te} - v_{0i})^2 \right] \frac{\theta^2 R_\rho}{8 \sin^2 \frac{\Phi}{2} R_L c_e^2} \right\} \quad (29)$$

In a compressible plasma in the thin slab limit, body modes can also propagate and their dispersion relation is given by

$$-\frac{4 \sin^2 \frac{\Phi}{2}}{\theta^2} \approx -q_i^2 + \frac{q_e^2}{R_L^2} + \left(S - \frac{1}{S}\right) \frac{q_i q_e}{R_L}, \quad (30)$$



Using the same method as in the case of surface waves, we obtain a dispersion relation of body waves in the thin slab approximation which is similar to the equation describing surface modes to the second order terms in Eqs. (28)–(29). Since the second order terms in these equations contain a term proportional to the very small  $\theta^2$ , changing the sign from plus (surface modes) to minus (body modes) will not affect our results significantly.

### 3 Waves in photospheric structures

A possible photospheric application would be the study of wave propagation in sunspots' penumbra. Viewed in white light, sunspots consist of a dark, central umbra surrounded by brighter, radially striated penumbra made up from alternating bright and dark filaments. Martinez Pillet (2000) suggested that these horizontal tubes might have diameters around 100 km.

The magnetic field in the umbra is vertical, but as soon as we approach the penumbra, the field lines tend to be horizontal, relative to the solar surface. Observations by Beckers and Schröter (1969) suggested that, while the magnetic field in the dark filaments is nearly horizontal, the field in the bright filaments is inclined to the horizontal with a mean inclination of  $10^\circ$ – $15^\circ$ . However, here we will suppose that in both types of filaments, the magnetic field is horizontal. Observations also showed that the magnetic field strength is weaker in dark regions than in the bright ones.

The plasma dynamics show a systematic inward (towards the umbra) plasma flow in the bright elements of the umbra and outward Evershed flow occurring mostly in the dark filaments. The most important motion in the penumbra is the radial, nearly horizontal (field aligned) outflow of plasma responsible for the Evershed effect seen in spectral lines formed in the penumbral photosphere. This motion is thought to be a siphon flow driven by a pressure difference between the footpoints of arched magnetic flux tubes. The siphon flow is probably also responsible for the reversed, inward Evershed flow seen higher up in the penumbral atmosphere, in chromospheric spectral lines such as  $H_\alpha$  (Schlichenmaier, 2002).

Radially outward propagating running penumbral waves have speeds of 10–20 km  $s^{-1}$ , repeating with a period in the range of 200–300 s with a horizontal wavelength of 2.3–3.8 Mm (Giovanelli, 1974). These propagation speeds are larger than the local sound speed, therefore they might be fast magnetoacoustic waves. Penumbral structures also support waves with periods around 5 min, which are related to the interaction of the sunspot with the resonant acoustic ( $p$ -modes) in the surrounding quiet Sun.

The possible modes arising in penumbral fine structures modelled as a periodic structure in the long wavelength limit (slender slab) are shown in Figures 3. Plots are obtained for three values of  $\Phi$  ( $\pi/10, \pi/2, \pi$ ) and three values of  $R_L$  (0.1, 2.5, 10). All characteristic speeds are normalized to the internal Alfvén speed.

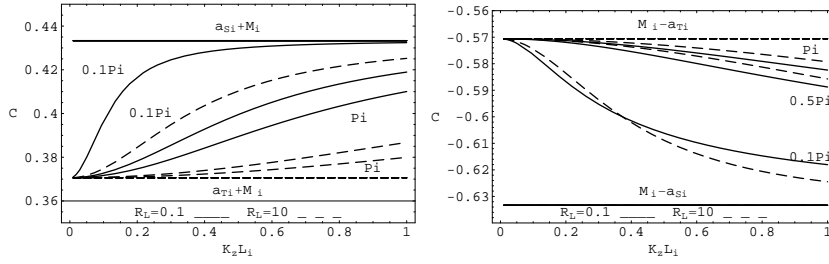


**Figure 3:** The phase speed of surface modes as a function of the dimensionless wavelength,  $\theta$  arising in a compressible periodic plasma (sunspot's penumbra). The solid lines correspond to  $R_L = 0.1$  and dashed lines to  $R_L = 10$ . ( $a = 0.8$ ,  $a_{S_i} = 0.533$ ,  $a_{T_i} = 0.47$ ,  $M_i = -0.1$  and  $M_e = 0.2$ )

With an Alfvén speed in bright regions of  $15 \text{ km s}^{-1}$ , we choose  $c_{S_i} = 9 \text{ km s}^{-1}$ ,  $c_{S_e} = 8 \text{ km s}^{-1}$  and  $v_{A_e} = 12 \text{ km s}^{-1}$ . For the equilibrium flow we choose Mach numbers such as  $M_i = -0.1$  and  $M_e = 0.2$ .

Since the ratio of the widths of two adjacent slabs appears in the dispersion relation, the dependence of the phase speed (in Alfvén speed units) with respect to  $R_L$  for a thin slab is shown in Figure 4.

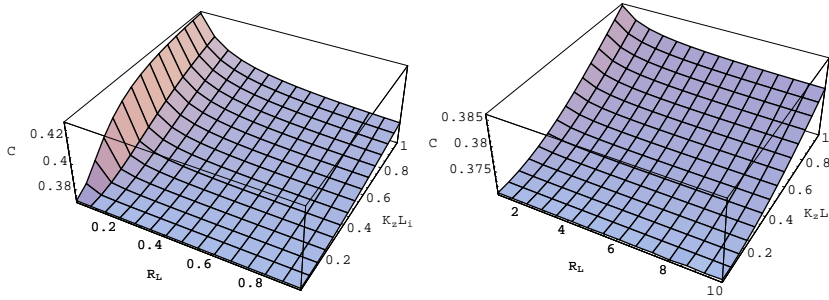


**Figure 4:** The phase speed of surface modes as a function of the dimensionless wavelength,  $\theta$ , and  $R_L < 1$  (left panel) and  $R_L > 1$  (right panel) in photospheric penumbrae.

The presented findings are preliminary results and a full investigation on the effect of equilibrium flows on the propagation of linear compressional MHD waves in periodic structures is underway. Part of this investigation will be the calculation of

the threshold for negative energy waves which can appear in these structures. Further models will be made for the plume/interplume system and the spaghetti structures in the solar wind.

### Acknowledgement

The authors acknowledge the financial support by the British Council and the Royal Society. One of the authors (IB) acknowledges the financial support by the Nuffield Foundation.

### References

- Athay, R.G. and Dere, D.P. 1991, *ApJ*, 381, 323  
Beckers, J.M. and Schröter, E.H. 1969, *Sol. Phys.*, 10, 384  
Berton, R. and Heyvaerts, J. 1987, *Sol. Phys.*, 109, 201  
Gabriel, A.H., Bely-Dubau, F. & Lemaire, P. 2003, *ApJ*, 589, 623  
Giovannelli, R.G. 1974, in R. Grant Athay (ed.) *Chromospheric Fine Structures*, IAU Symp., 56, 137  
Hollweg, J.V. 1982, *J. Geophys. Res.*, 87, 8065  
Hollweg, J.V. and Roberts, B. 1984, *J. Geophys. Res.*, 89, 9703  
James, S.P. and Erdélyi, R. 2002, *A&A*, 393, L11  
Roberts, B. 1979, *Sol. Phys.*, 61, 23  
Roberts, B. 1981, *Sol. Phys.*, 69, 27  
Ruderman, M.S., Roberts, B., Pelinovsky, E.N. and Petrukhin, N.S. 2001, *Phys. Plasmas*, 8, 2628  
Martinez Pillet, V. 2000, *A&A*, 361, 734  
Nakariakov, V.M and Roberts, B. 1995, *Sol. Phys.*, 159, 213  
November, L.J., Toomre, J., Gebbie, K.B. and Simon, G.W. 1979, *ApJ*, 227, 600  
Schlichenmaier, R. 2002, *Astron. Nachrichten*, 323, 303  
Spruit, H.C. 1981, in *The Sun as a star*, ed. Jordan, S.D. *NASA Spec. Publ.*, 450, 385  
Uralov, A.M. 2003, *Sol. Phys.*, 218, 17  
Winebarger, A. R., Warren, H., van Ballegoijen, A., DeLuca, E.E. & Golub, L. 2002, *ApJ*, 567, L89